



Marsh benthic Foraminifera response to estuarine hydrological balance driven by climate variability over the last 2000 yr (Minho estuary, NW Portugal)



João Moreno ^{a,*}, Francisco Fatela ^a, Eduardo Leorri ^b, José M. De la Rosa ^c, Inês Pereira ^{d,1}, M. Fátima Araújo ^d, M. Conceição Freitas ^a, D. Reide Corbett ^b, Ana Medeiros ^d

^a Universidade de Lisboa, Faculdade de Ciências, Centro de Geologia, Departamento de Geologia, Campo Grande, 1749-016 Lisboa, Portugal

^b East Carolina University, Department of Geological Sciences, Greenville, NC 27858-4353, USA

^c Instituto de Recursos Naturales y Agrobiología de Sevilla, Av. Reina Mercedes 10, 41012 Sevilla, Spain

^d Universidade de Lisboa, Instituto Superior Técnico, Centro de Ciências e Tecnologias Nucleares, Estrada Nacional 10, km 139,7, 2695-066 Bobadela LRS, Portugal

ARTICLE INFO

Article history:

Received 26 June 2013

Available online 14 July 2014

Keywords:

Marsh foraminifera
Hydrological balance
Palaeoenvironmental reconstruction
Climate variability
RWP to Present
Minho estuary
NW Iberian region

ABSTRACT

A high-resolution study of a marsh sedimentary sequence from the Minho estuary provides a new palaeoenvironmental reconstruction from NW Iberian based on geological proxies supported by historical and instrumental climatic records. A low-salinity tidal flat, dominated by *Trochammina salsa*, *Haplophragmoides* spp. and *Cribrostomoides* spp., prevailed from AD 140–1360 (Roman Warm Period, Dark Ages, Medieval Climatic Anomaly). This sheltered environment was affected by high hydrodynamic episodes, marked by the increase in silt/clay ratio, decrease of organic matter, and poor and weakly preserved foraminiferal assemblages, suggesting enhanced river runoff. The establishment of low marsh began at AD 1380. This low-salinity environment, marked by colder and wet conditions, persisted from AD 1410–1770 (Little Ice Age), when foraminiferal density increased significantly. *Haplophragmoides manilaensis* and *Trochammina salsa* mark the transition from low to high marsh at AD 1730. Since AD 1780 the abundances of salt marsh species (*Jadammina macrescens*, *Trochammina inflata*) increased, accompanied by a decrease in foraminiferal density, reflecting climate instability, when droughts alternate with severe floods. SW Europe marsh foraminifera respond to the hydrological balance, controlled by climatic variability modes (e.g., NAO) and solar activity, thus contributing to the understanding of NE Atlantic climate dynamics.

© 2014 University of Washington. Published by Elsevier Inc. All rights reserved.

Introduction

Tidal marshes are dynamic ecosystems, considered critical transition zones between adjacent terrestrial and marine environments within the estuarine landscape. These environments have been the source of considerable benefits, both social and economic. The human impact on tidal marshes started a long time ago (e.g., drainage and agriculture, grazing, saltpans), and increased in modern times (dredging, harbors, heavy industries, communication routes and urban settlement, agriculture, sewages and industrial effluents). Identifying past environmental changes that influenced the estuarine margins, whether triggered by natural internal processes (e.g., sediment supply), external forcing (e.g., solar irradiance, volcanic aerosols, atmospheric circulation patterns)

or by persistent human impact (e.g., anthropogenic induced climate warming), is essential to understand global and regional climatic variability and the relationship between climate and sea level during the last two millennia.

Since the pioneering works of Phleger (1965) and Scott and Medioli (1978, 1980), tidal marsh foraminiferal assemblages have been used as palaeoenvironmental proxies and sea-level indicators in Holocene intertidal deposits (e.g., Gehrels, 1994; Hayward et al., 1999; Horton, 1999; Scott et al., 2001; Gehrels and Newman, 2004; Horton and Edwards, 2005; Fatela et al., 2009; Leorri et al., 2010a, 2011). The distribution of foraminiferal species across tidal marshes around the world exhibits a vertical zonation with respect to the tidal frame that depends on abiotic and biotic factors and allows the recognition of foraminiferal assemblage characteristics of a narrow zone (high marsh) between mean high water (MHW) and mean high water spring (MHWS). They also provide an efficient method to reconstruct water circulation patterns in estuaries and the interplay between marine and freshwater inflow (e.g., Hayward et al., 1999; Leorri and Cearreta, 2009a). The study of modern foraminiferal patterns can be used to interpret fossil brackish

* Corresponding author. Fax: +351 21 750 01 19.

E-mail address: jcmoreno@fc.ul.pt (J. Moreno).

¹ Present address: LIRIO – Pólo de Estremoz da Universidade de Évora, Convento das Maltezas, 7100-513 Estremoz.

foraminiferal faunas and they are of special relevance to recent methods of determining rates of Quaternary changes in sea level, climate and geohistory (e.g., Hayward et al., 1999; Hippensteel et al., 2005; Alday et al., 2006; Drago et al., 2006; Horton and Murray, 2006; Horton and Culver, 2008; Leorri and Cearreta, 2009b; Leorri et al., 2013).

In the present work, foraminiferal data are combined with both descriptive documental records and instrument-based observations (i.e., meteorological and hydrological) to improve the understanding of climate variability in the NW of Portugal over the last 2000 yr. Further comparison with historical climatic information from the Iberian Peninsula (e.g., Font, 1988; Benito et al., 1996, 2008, 2010; Bernárdez et al., 2008a; Martín-Chivelet et al., 2011) and palaeoclimatic reconstructions from offshore Atlantic Iberian margin (Lebreiro et al., 2006; Rodrigues et al., 2009; Abrantes et al., 2011) was made to recognize and characterize the potential of marsh foraminiferal assemblages as a proxy for major shifts in climate. Notwithstanding the uncertainties inherent to the dating methods, especially sub-centennial scale chronologies based on radiocarbon dating, foraminiferal changes over the last two millennia might reflect climatic changes such as Roman Warm Period (RWP), Dark Ages (DA), Medieval Climatic Anomaly (MCA), Little Ice Age (LIA), the Solar activity cycles (maxima and minima), the present warming pulse, as well as extreme climatic events.

Study area

The Minho River runs through the NW of Portugal (Fig. 1), defining 77 km of the political border with Spain, just before reaching the Atlantic Ocean near the ancient fortress town of Caminha. It drains a carbonate depleted Variscan basement across the rainiest area of Portugal, with an average annual precipitation of 1780 mm (maxima 3470 mm; <http://snirh.pt>). The annual average fluvial discharge is approximately

300 m³/s and the winter peak discharge (December to March) generally exceeds 1000 m³/s; the 100-yr flood recorded 6100 m³/s (Bettencourt et al., 2003). In spite of the construction of several dams since AD 1951, a correlation between river flow and precipitation of $R = 0.85$ (Fatela et al., 2013) to $R = 0.88$ (Gómez-Gesteira et al., 2011) was found in Minho, as well as a correlation between winter precipitation and NAO index of $R = 0.70$ (Fatela et al., 2013).

The Minho estuary presents a semi-diurnal high-mesotidal regime where astronomical tides range between 2 m and almost 4 m under neap or spring waters, respectively. However, tidal levels are often amplified by storm surges (Taborda and Dias, 1991). The dynamic tide is felt up to 40 km upstream (Alves, 1996). The upstream limit of marine water is recorded up to 6–9 km (Fatela et al., 2009). This estuary is shallow, as a result of widespread siltation, and semi-enclosed by a mouth bar, exposing a considerable part of the bottom during low water spring tide. The lower estuary extends a few kilometres from the mouth and behaves as “partially mixed” (Brown et al., 1991; Moreno et al., 2005c). The most extensive marsh development occurs in the south bank of the Minho estuary, at the confluence with the Coura River (hereafter referred to as the Caminha tidal marsh), providing an adequate site to investigate the current and past distribution of foraminiferal assemblages (Fig. 1).

Surface foraminiferal distribution at Caminha marsh

Several studies related to the living and dead marsh foraminiferal assemblage zonation and their environmental constraints (Moreno et al., 2005a, 2005b, 2005c, 2006, 2007; Fatela et al., 2007, 2009) and Holocene sea-level changes (Leorri et al., 2010a, 2011, 2013) have been carried out. The main control to the general composition of the foraminiferal assemblages is salinity and submersion time (e.g., Fatela

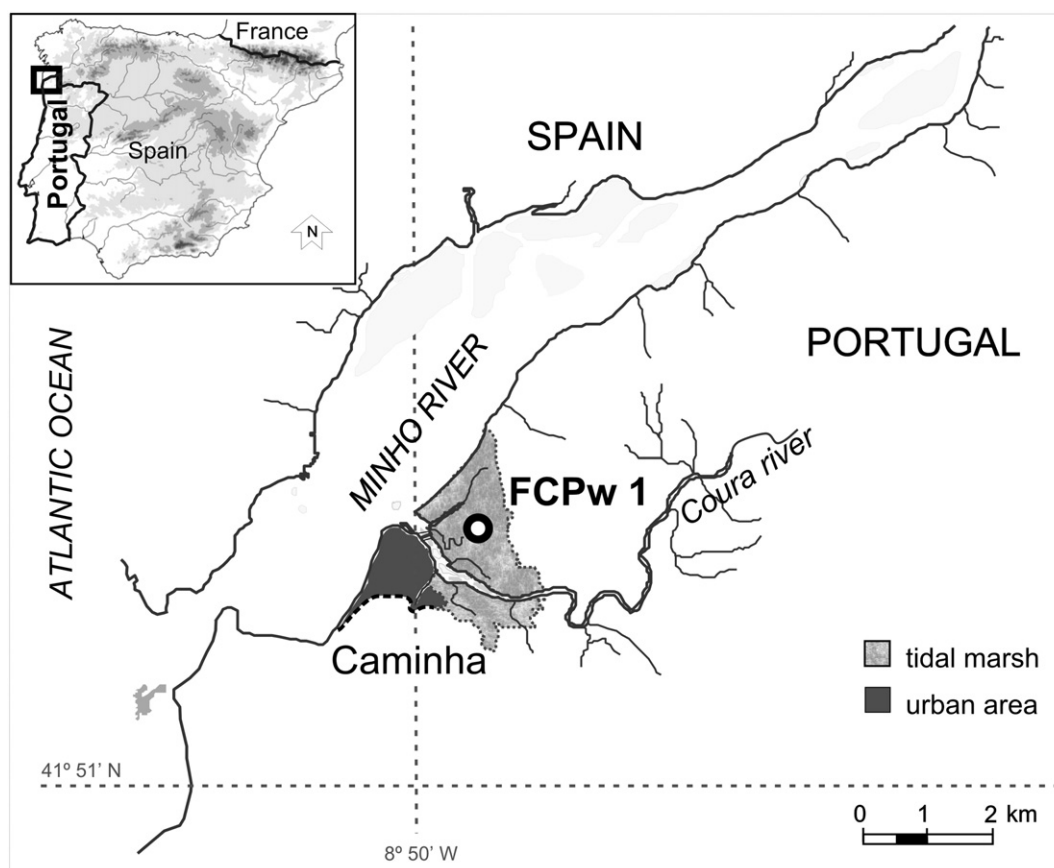


Figure 1. Location of core FCPw1 in the Caminha tidal marsh (Minho estuary, NW Portugal).

et al., 2009). However, these assemblages are also controlled by calcite undersaturation in these brackish marshes and tidal flats, where marine water is the major source of carbonates (Moreno et al., 2007; Valente et al., 2009). While with each tidal cycle salinity present large changes, foraminifera live infaunally (i.e., inhabit the sediment) and the controls are exerted by interstitial pore water that buffer these drastic changes (Fatela et al., 2009). The particular conditions (e.g., undersaturation in calcite, low pore-water pH) of the interstitial water have led to foraminiferal assemblages strongly dominated by robust agglutinated foraminifera, since calcareous foraminifera dissolve and most fragile marsh agglutinated tests disaggregate in response to these geochemical conditions.

Low-salinity conditions limit the elevation at which foraminiferal assemblages can be found. In fact, in this region the typical highest high marsh zone is absent and it is instead colonized by terrestrial vegetation. A pronounced dilution of marine water, caused by plentiful rain, in conjunction with the morphology of the estuary, limits the tidal salt wedge penetration landwards and residence time of marine waters within the estuarine space.

Following the tidal marsh foraminiferal zonation previously defined by the seminal work of Scott and Medioli (1980), a study of forty-eight surface sediment samples (from the Spring and Fall of 2002; Fatela et al., 2009), shows that Caminha assemblages from the high marsh IB sub-zone, between mean high waters (MHW) and mean high waters spring (MHWS), are dominated by *Haplophragmoides* sp. and *Haplophragmoides manilaensis* (Andersen, 1953), together with *Pseudothurammmina limnetis* (Scott and Medioli, 1980) as a co-dominant species in the living assemblage. The low marsh zone II is characterized by the dominance of *Miliammina fusca* (Brady, 1870). This zone may be subdivided into a IIA upper subzone, between MHW and mean high waters neap (MHWN), where *M. fusca* is accompanied by secondary species *P. limnetis*, and a lower subzone IIB defined by *M. fusca* and secondary *Psammospaera* sp. This subzone is located between MHWN and the mean tide level (MtL, i.e., mean water level inside the estuary). *Haplophragmoides manilaensis* characterises the elevation range between MHW and MHWS (0.99 m to 1.11 m above Minho estuarine MtL). It is the most abundant in both the living (stained) and dead assemblages. Because of its dominance and limited vertical range, *H. manilaensis* is an important sea-level and low-salinity high marsh indicator (Fatela et al., 2009).

A new set of eighteen surface samples was collected in May 2010 to improve the understanding of the Caminha high marsh assemblage (Fatela et al., 2013). Correspondence Analysis (CA) integrating dead benthic foraminiferal results from both the 2002 and 2010 samples resulted in 3 defined groups according to foraminiferal assemblage distribution across the tidal marsh zonation, with a significant correlation with submersion time (Fatela et al., 2013). However, a difference is evident between the two sampling periods when the dominant salt marsh species are evaluated; for instance, *Trochammina inflata* (Montagu, 1808) and *Jadammina macrescens* (Brady, 1870) were absent in 2002 but are common in 2010. This decline of lower salinity species (*Haplophragmoides* sp., *H. manilaensis*, *H. wilberti* and *P. limnetis*) abundances is seen as a direct consequence of the salinity increase of the interstitial water in the marsh, which reflects a decrease in the regional precipitation regime during the 8 yr that separate the samplings (Fatela et al., 2013). This observation points out that the records of benthic foraminifera from Caminha high marsh represent an important proxy for high-resolution studies of climate variability (Fatela et al., 2013).

Materials and methods

The Caminha high marsh sediment core FCPw1 was collected with a manual auger sampler (5 replicated cores, one meter long each) at 1.55 m above mean sea level (41° 52' 37" N and 8° 49' 28" W; Fig. 1), and transferred to a half PVC pipe and wrapped with cling film to protect it during transport and minimize desiccation.

Foraminifera

In the laboratory, the core was carefully sliced into 1-cm intervals and 56 samples (ca. 25 cm³) were analysed for foraminiferal purposes. Samples were taken every centimeter to a depth of 30 cm, below which samples were collected every other cm down to 50-cm depth and alternating 2 cm from 50 cm to the core bottom. Each sample corresponds to a circular slice of sediment with a volume of ca. 25 cm³. Samples were wet sieved to remove clay and silt material (63 µm mesh). At least 100 individuals were wet picked with a micropipette in each sample, a number fully adequate to characterize the low-diversity assemblages of tidal marshes (Fatela and Taborda, 2002). When the number of specimens was too low, the trichloroethylene (density = 1.46 g/cm³) flotation procedure was used to separate foraminiferal tests from sand particles (Murray, 2006). All specimens contained in that fraction were picked.

Foraminiferal identification followed Loeblich and Tappan (1988) to generic classification and several published papers regarding tidal marsh foraminifera for specific classification (e.g., Murray, 1971; Scott and Medioli, 1978, 1980; Hayward et al., 1999; Debenay et al., 2002). The specimens picked per sample were archived in a microplaqueontological Plummer cell slide.

Sedimentology and geochemistry

Two replicate cores were sliced every centimeter for geochemical and sedimentological purposes. All samples were frozen and then freeze-dried prior to the analyses. Organic matter (OM) content was determined by loss on ignition methodology (LOI), using a 2 g of bulk sediment dried and oven-heated at a temperature range of 490–510°C, for about 2 h. Sediment pH was determined using the electrometric method (Head, 1980) with an inoLab WTW series pH730 model. Wet sieving was used to separate and determine the ratio of coarse (>63 µm):fine (<63 µm) particles, and the silt and clay fractions were determined using a Malvern laser particle analyzer and Mastersize2000 software. Selected samples of one of the replicates were sieved to remove the coarser particles larger than 2 mm. The remaining material (<2 mm) was dried, ground in an agate mill, and a portion was homogenized and compacted into pressed pellets for analysis by Energy-Dispersive X-Ray Fluorescence Spectrometry (EDXRF) using a KEVEX 771 spectrometer. Spectral data were acquired for the quantification of Al, Si, S, Cl, K, Ca, Ti, Cr, Mn, Fe, Ni, Cu, Zn, Br, Rb, Sr, Zr, and Pb. A detailed description on the sample preparation, analytical conditions, detection limits and the accuracy and precision of the overall procedure has been published elsewhere (Araújo et al., 1998, 2003). In this multi-proxy analysis, special focus was made on the elements recognized as proxies of marine and continental inputs.

Chronology

The upper section of the core was dated via ²¹⁰Pb measured by alpha spectroscopy following the methodology of Nittroer et al. (1979). In this approach, unsupported ²¹⁰Pb (²¹⁰Pb_{Excess}) is determined as the difference of ²¹⁰Pb activity versus ²²⁶Ra, assumed to be in equilibrium at depth within the core (Nittroer et al., 1979). ¹³⁷Cs (Smith, 2001) and total Pb activities (Leorri et al., 2008; Leorri and Cearreta, 2009b) were used to support the ²¹⁰Pb-derived chronology based on the constant rate of supply model (CRS; Appleby and Oldfield, 1992), as it has been shown to be the most suitable for the region (Leorri et al., 2010b). The radionuclide ¹³⁷Cs was determined by its gamma emissions at 662 KeV (Appendix A). Samples were counted for 24 h to the depth of limit of measurable fallout ²¹⁰Pb or ¹³⁷Cs, i.e., until activity concentrations of both radionuclides dropped below the minimum detectable activity (Leorri et al., 2010b). Six additional samples (40–41 cm, 44–45 cm, 63–64 cm, 66–67 cm, 81–82 cm and 90–91 cm depth) were analysed for radiocarbon content (total organic) at Beta Analytic Inc.

(USA) (Table 1) to extend the chronology downcore (Fig. 2). The interpolation of the data has been performed using a Bayesian age-depth model (Bchron 3.2; Haslett and Parnell, 2008; Parnell et al., 2008) to provide age and associated errors to the environmental reconstructions. The lowermost 10 cm (91–100 cm depth) has been extrapolated by linear regression from the Bchron calculation between 81 and 91 cm depth. This section has to be considered carefully as errors cannot be calculated. The obtained calendar ages are presented in years of *Anno Domini* (AD).

Historical and instrumental records

The last two millennia comprise five well-known climatic historical periods: 1) Roman Warm Period (RWP, AD 0–400; e.g., Lamb, 1985); 2) Dark Ages Cold Period (DA, AD 400–700; e.g., Keigwin and Pickart, 1999); 3) Medieval Climatic Anomaly (MCA, AD 900–1300; e.g., Stine, 1994; Mann et al., 2009; Trouet et al., 2009; Cook et al., 2010; Graham et al., 2011); 4) Little Ice Age (LIA, AD 1350–1900; e.g., Bradley and Jones, 1993) and 5) 20th century warming (present warm period – PWP), as recorded by instrumental temperature measurements over the last two centuries. These climate changes were also recognized by several authors that have studied the variability of the climatic conditions in Northern Iberian Peninsula during the late Holocene until present using proxies like organic and inorganic geochemistry, sedimentology and micropalaeontology (e.g., Martínez Cortizas et al., 1999; Luque and Juliá, 2002; Desprat et al., 2003; Pla and Catalan, 2005; Lebreiro et al., 2006; Burdloff et al., 2008; Martín-Chivelet et al., 2011; González-Álvarez, 2013). In addition, several extreme local climatic events, like strong flooding episodes, are documented (e.g., Marquina, 1949; Benito et al., 1996, 2008; Abrantes et al., 2011). These events have typically occurred at times of transition between climatic periods (e.g., AD 500–600, AD 1100–1200, AD 1450–1600). For example, alternating periods of intensive precipitation and thunderstorms with severe droughts were common during the 18th and 19th centuries as recorded in Portugal (e.g., Marques, 2001; Do Ó and Roxo, 2008; Pfister et al., 2010) and several localities from southern and northern Spain (e.g., Riera et al., 2004; Llasat et al., 2005; Vicente-Serrano and Cuadrat, 2007; Benito et al., 2008, 2010; Domínguez-Castro et al., 2008; Gil-García et al., 2008; Martín-Puertas et al., 2008).

Solar activity cycles (maxima and minima) are based on Versteegh (2005), Usoskin et al. (2007), Scaffeta (2012), Steinhilber et al. (2012), WDC and NOAA (2013). Precipitation data were compiled from the monthly records of meteorological stations from the Minho region since 1930. The available data from the Portuguese sectors of Minho and Lima basins were merged in order to obtain the longest and the most representative record of the area (<http://snirh.pt>). This series of precipitation data from 1932 to 2010 was used to compute the SPI (McKee et al., 1993; Moreira et al., 2012) with a freeware program (SPI_SL_6.exe) available at the National Drought Mitigation Center of the University of Nebraska–Lincoln (<http://drought.unl.edu>). The SPI allows the identification of drought events and classifies their severity according to defined drought classes. The wide use of this index comes

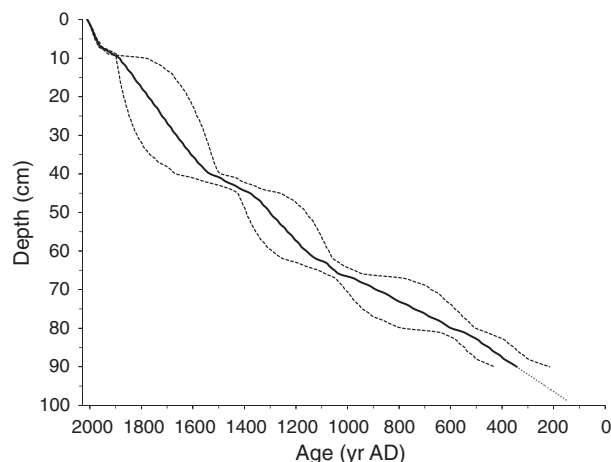


Figure 2. Age model for the core FCPw1 and estimated 2σ errors, based on six AMS-¹⁴C dates, performed on total organic sediment, and ²¹⁰Pb chronology. The data interpolation was obtained with Bchron 3.2 software. The lowermost 10 cm has been extrapolated from the Bchron calculation between 81 and 91 cm depth by linear regression.

from its reliability and relatively easy comparison between different locations and climates (<http://drought.unl.edu>). Moreira et al. (2012) determined the SPI from Porto (Serra do Pilar: 41° 08' 19.20" N–08° 36' 09.68" W), ca. 80 km south of Caminha, based on the precipitation record from 1863 to 2007. Considering the good correlation (R = 0.85) between SPI from Minho region and Porto, the latter was used as representative of severe and extreme droughts that occurred in NW Portugal. In this work, the SPI 12 month period was used because it reflects long-term precipitation patterns and identifies dryer periods of long duration with impact in the hydrological regime (e.g., McKee et al., 1993; Moreira et al., 2012; <http://drought.unl.edu>). The identification of the severe and extreme drought periods between 2007 and 2010 in NW Portugal was completed with the on-line SPI data provided by the Instituto Português do Mar e da Atmosfera (IPMA, 2013).

Results

Based on foraminiferal assemblages (defined in terms of species presence, abundance, dominance and density – number of foraminifera per cm³; Appendix B), the Caminha marsh core (FCPw1) can be divided into six different Foraminiferal Assemblage Zones (FAZ VI to I; Table 2). This division is also supported in sedimentological and geochemical data (Table 2, Appendix C).

FAZ VI (100 cm to 46 cm depth) ranges from AD 140 to 1380, encompassing the RWP, DA cold period and the MCA. The foraminiferal assemblages are scarce (average 3 tests/cm³), often exhibiting poorly preserved tests and low diversity (average 3 species/sample). Assemblages are composed primarily by the upstream low-salinity species *Trochammina salsa/irregularis* (Cushman and Brönnimann, 1948), followed by *Cribrostomoides* spp. and *Haplophragmoides* spp (Table 2). *Jadammina macrescens* is also present (7%) at AD 1070.

Sediment is essentially mud (average 97%) and the OM content ranges between 6% and 13%; the pH values are generally low, exhibiting an average of 4.8 (Table 2; Appendix C); the higher concentration of Zr is recorded in this FAZ (average 213 ppm; Appendix C). In this zone, some interval barren of foraminifera tend to be related with higher silt/clay ratio (Appendix B and C), namely at AD 190, 800, 1140, 1270 and two in the interval AD 1310–1340.

FAZ V (46 cm to 29 cm depth) ranges from AD 1380 to 1690 and is included within the LIA period. This unit records a strong increase in the density of the assemblages (average 260 tests/cm³), but low species richness remains (average 5 species/sample). The low-salinity species still dominate (82–95%), namely *T. salsa/irregularis* and *M. fusca*, with minor presence of *Haplophragmoides* spp, *Cribrostomoides*

Table 1 Radiocarbon ages data determined in the Laboratory "Beta Analytic Inc.". (AMS – standard delivery).

Sample	Depth (cm)	δ ¹³ C ‰	Conventional radiocarbon age	Δ14C ‰	Calibrated years AD (2 sigma range)
CM 41	40–41	–26.7	380 ± 30 BP	–46.20 ± 3.6	1490 to 1666
CM 45	44–45	–26.8	650 ± 35 BP	–84.57 ± 3.9	1330 to 1453
CM 64	63–64	–25.9	1010 ± 50 BP	–122.49 ± 1.9	1032 to 1197
CM 67	66–67	–25.9	1030 ± 34 BP	–124.97 ± 1.9	934 to 1082
CM 82	81–82	–25.8	1570 ± 40 BP	–181.66 ± 1.9	463 to 650
CM 91	90–91	–27.2	1760 ± 30 BP	–196.80 ± 3.0	215 to 429

²¹⁰Pb CRS chronology supported by ¹³⁷Cs and total Pb concentrations of Caminha high marsh sediment core (FCPw 1) are available in Appendix A.

Table 2
Summary of micropaleontological and sedimentological data. The values represent the average (bold) and the range; Low Sal. spp. % – low-salinity species group; Salt marsh spp. % – “normal” salinity species group; NF – number of foraminifera; S – number of species; assemblages dominant species (bold).

FAZ	Depth cm	Age yr AD	Benthic foraminifera %	Low sal. spp. %	Salt marsh spp. %	NF/cm ³	S	pH	OM %	Mud %
I	0–4	2010 1985	H. manilaensis (49; 40–56); Haplophragmoides spp (23; 2–65), M. fusca (12; 2–20) and T. salsa/irregularis (9; 7–11), <i>Cribrostomoides</i> spp.(5; 210), <i>T. inflata</i> (7; 2–13); <i>H. wilberti</i> , <i>P. limnetis</i> , <i>T. comprimata</i> , <i>J. macrescens</i> and <i>P. guaratibaensis</i> ≤5	84 77–88	12 8–21	253 22–498	9 7–11	5.1 4.6–5.4	53 46–65	63 50–69
II	4–10	1985 1900	H. manilaensis , (35; 16–63), T. salsa/irregularis (11; 4–15), M. fusca (6; 5–6), associated with T. inflata (12; 3–41), J. macrescens (11; 3–14), <i>T. comprimata</i> (4; 1–8) <i>H. wilberti</i> (8; 4–13); <i>P. guaratibaensis</i> , <i>S. lobata</i> and <i>P. limnetis</i> ≤5	58 36–78	37 14–59	168 68–252	9 7–10	5.4 5.1–5.7	38 36–40	74 51–88
III	10–20	1900 1780	H. manilaensis (32; 21–51), T. salsa/irregularis (19; 10–32), M. fusca (4; 1–8), Haplophragmoides spp (46); <i>J. macrescens</i> (17; 12–23), <i>T. inflata</i> (12; 3–22), <i>T. comprimata</i> (7; 3–13); <i>Cribrostomoides</i> spp., <i>H. wilberti</i> , <i>P. guaratibaensis</i> , <i>P. ipohalina</i> and <i>P. limnetis</i> ≤5	57 44–78	35 10–47	79 17–205	8 6–9	5.7 5.7–5.8	33 22–40	79 66–88
IV	20–29	1780 1690	T. salsa/irregularis (59; 16–74), H. manilaensis , (26; 6–63), M. fusca (5; 1–16); <i>Cribrostomoides</i> spp., <i>H. wilberti</i> , <i>P. limnetis</i> and <i>T. comprimata</i> , <i>J. macrescens</i> , <i>T. inflata</i> , <i>P. guaratibaensis</i> , <i>P. ipohalina</i> ≤5	91 84–95	4 1.3–11	244 161–345	6 4–9	5.8 5.7–5.9	30 25–38	86 81–90
V	29–46	1690 1380	T. salsa/irregularis (77; 74–92), M. fusca (7; 1–16), <i>Haplophragmoides</i> spp (4; 0.7–12), <i>Cribrostomoides</i> spp. (4; 0.8–9), <i>T. comprimata</i> (4; 0.7–6); <i>H. manilaensis</i> , <i>P. limnetis</i> , <i>P. guaratibaensis</i> , <i>S. lobata</i> , <i>J. macrescens</i> , <i>T. inflata</i> , <i>P. ipohalina</i> ≤5	88 82–95	4 1.4–9	260 63–609	5 4–8	6.1 5.8–6.6	19 12–24	91 80–95
VI	46–100	1380 140	T. salsa/irregularis (59; 21–80), Cribrostomoides spp. (14; 2–42), Haplophragmoides spp (10; 4–26), <i>J. macrescens</i> (3; 1–7); <i>M. fusca</i> , <i>T. Inflata</i> , <i>P. ipohalina</i> ≤5	76 59–88	3 0.8–8	3 0.1–13	3 2–5	4.8 3.8–6.7	8 6–13	97 93–100

sp., *H. manilaensis* and *P. limnetis*. Salt marsh species *Tiphrotrocha comprimata* (Cushman and Brönnimann, 1948), *Paratrochammina guaratibaensis* (Brönnimann, 1986), *Polysaccammina ipohalina* Scott, 1976, and *Siphrotrochammina lobata* (Saunders, 1957) join *J. macrescens*, and *T. inflata* (Table 2; Appendix B).

Concomitant with FAZ V, mud percentage decreases (average 91%) while OM content (12% to 24%) and pH values (average 6.1; Table 2) increase; the average concentration of Zr falls in this zone to 161 ppm, whereas Br exhibits an opposite trend rising from an average content of 148 ppm (FAZ VI) to 483 ppm (FAZ V; Appendix C).

The FAZ IV (29 cm to 20 cm depth) spans from AD 1690 to 1780 (LIA). Foraminifera in this unit are still abundant (average 244 tests/cm³). The assemblages have low diversity (average 6 species/sample) and they are still dominated by low-salinity species (84–95%), *T. salsa/irregularis*, *H. manilaensis* and *M. fusca*, along with secondary species *Cribrostomoides* sp., *H. wilberti* and *P. limnetis* (Table 2). Salt marsh foraminifera, *T. comprimata*, *J. macrescens*, *T. inflata*, *P. guaratibaensis* and *P. ipohalina*, are also found. The increasing trend of OM towards the top of the core is significant, reaching 25–38% in this FAZ (Table 2). Likewise, the sediment texture continues the tendency of coarsening towards the top of the core (average mud percentage 86%), but the coarse fraction is mainly represented by plant debris. Br presents its highest content, with 1300 ppm (average 927 ppm), and the concentration of Zr continues falling in this FAZ (average 143 ppm; Appendix C).

FAZ III (20 cm to 10 cm depth) extends between AD 1780 and 1900 (LIA). Low foraminiferal diversity (8 species/sample) prevails and density exhibits a significant drop (average 79 tests/cm³). Low-salinity species (*H. manilaensis*, *T. salsa/irregularis*, *M. fusca* and *Haplophragmoides* spp.) dominate (average 57%), but in this FAZ the “normal” salinity species (*J. macrescens*, *T. inflata* and *T. comprimata*) become a significant part of the assemblages (average 35%). Minor species are represented in this FAZ by *Cribrostomoides* spp., *H. wilberti*, *P. guaratibaensis*, *P. ipohalina* and *P. limnetis* (Table 2). The OM content remains high (average 33%) and the average mud content decreases to 79% (Table 2). Br still exhibits high concentration (average 605 ppm).

FAZ II (10 cm to 4 cm depth) spans from AD 1900 to 1985 (PWP). Foraminiferal assemblages reach the highest number of species (9), but have similarly low diversity and exhibit a consistent density increase, with an average of 168 tests/cm³. Low-salinity species represent

58% (average) of the assemblages and “normal” salinity species 37% (average; Table 2). This FAZ records the only interval (8–9 cm; AD 1934) where “normal” salinity species became dominant (59%), marked by the acme of *T. inflata*. Mud percentage and Zr sediment content present the same trend as in the previous FAZ III, while OM and Br content increase, the latter achieving the average of 919 ppm (Table 2; Appendix C).

FAZ I (4 cm to 0 cm depth), from AD 1985 to 2010, shows that diversity of foraminiferal assemblages is still low until present (maximum 11 species) but their density increases to an average of 253 tests/cm³ (Table 2). The lower faunal densities occur between AD 1995 (22 tests/cm³) and AD 2002 (99 tests/cm³). In this FAZ, the high marsh foraminiferal assemblages are dominated by the low-salinity species *H. manilaensis*, *Haplophragmoides* spp., *M. fusca* and *T. salsa/irregularis*, representing 77% to 88% of the assemblage, with *Cribrostomoides* spp., *H. wilberti* and *P. limnetis* as minor representatives as well as the “normal” salinity marsh species *T. comprimata*, *J. macrescens*, *P. guaratibaensis*. *Trochammina inflata* is the most representative of this group (average 7%; Table 2), reaching the highest percentages at the uppermost sample (AD 2010), although its presence is significantly reduced from FAZ II to FAZ I. The coarsening upwards trend is clear in FAZ I (average 63% mud), as well as the increase of OM content (average of 53%), reflecting the observed increase of marsh plant debris. Zr and Br trends change, with the gradual decrease of Zr from the bottom to the top of the core (average 115 ppm) and the Br content increasing to an average of 1120 ppm (Appendix C).

Discussion

The sediment texture of core FCPw1 and the OM content (Table 2) indicate the development of a tidal flat (FAZ VI) that lasted over 1200 yr (AD 140–1380). During this period, foraminiferal assemblages present low density, with a dominance of few low-salinity species (Fig. 3). However these originally scarce assemblages, like in the tidal flats modern analogs (Fatela et al., 2009), are often poorly preserved, suggesting a diagenetic alteration, probably related to the low values of sediment pH (Table 2) that seem to reflect a strong fluvial influence. In fact, minimum pH values of 4.33 have been recently measured in the Coura river waters (Moreno et al., 2005a). Alternatively, foraminifera

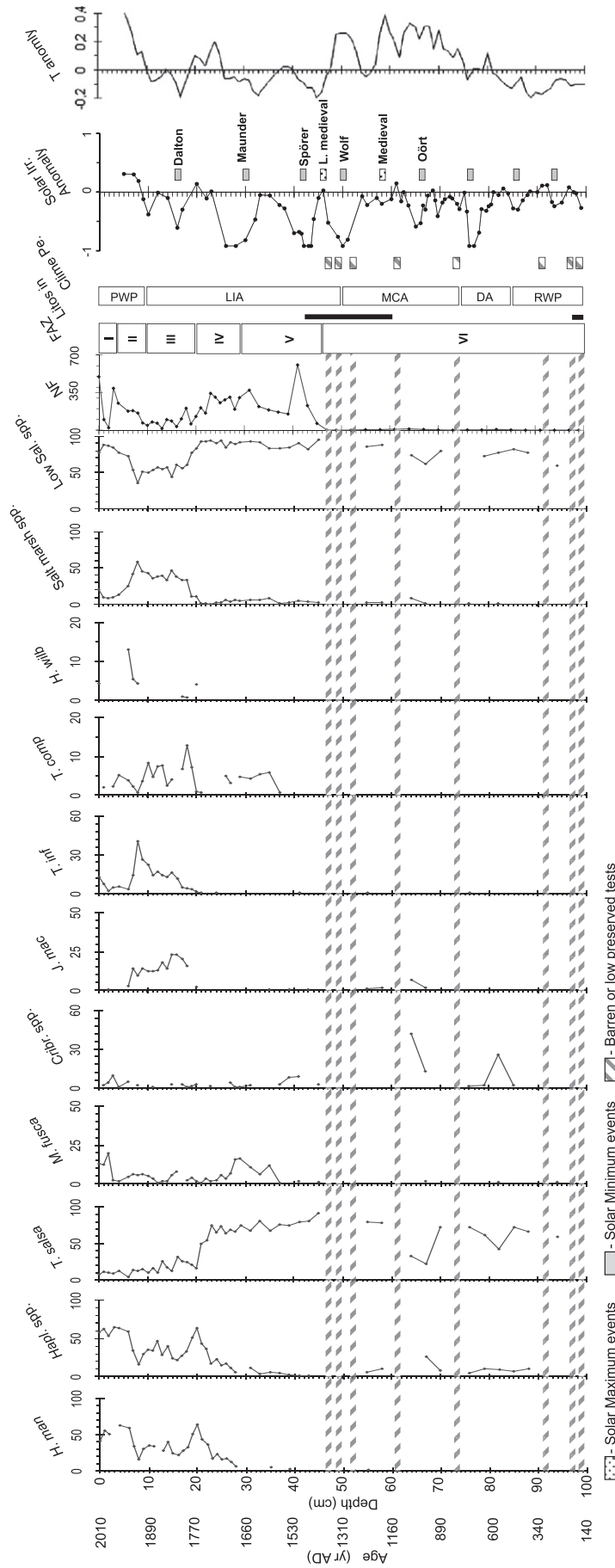


Figure 3. Percentage distribution of benthic foraminifera in core FCPw1. Age (yr AD) — age in calendar years AD; Salt marsh spp. — distributions of the group of low-salinity benthic species; NF — number of foraminifera per cm³; FZ — foraminiferal assemblage zones; LIA — periods of continental lithogenic inputs to the shelf (see references in the text and Appendix E); Clime Pe. — climate periods in the last 2 millennia (see references in the text); Solar Irr. Anomaly — solar irradiance anomaly using a 22-yr running average reconstruction (after Steinhilber et al., 2012); Solar Ev. — solar events (see references in the text); T anomaly — temperature anomaly using a 10-yr running average reconstruction (after Martín-Chivelet et al., 2011).

are absent from this depositional setting probably due to low salinity. These low abundances tend to be correlated with higher silt/clay ratio (Fig. 4). Silt/clay ratio could be used as a proxy of hydrodynamic energy, where higher silt content could be associated to periods of rainfall/flood intensification, mainly at AD 140–190, AD 320 and AD 800, AD 1140, AD 1270 and AD 1310–1340. Desprat et al. (2003) identified the development of temperate vegetation during Roman colonization in Galicia (RWP, peaking at AD 150), suggesting that this period presented humid conditions. Moreover the palaeotemperature records from speleothem materials located in the North of Spain (Martín-Chivelet et al., 2011) show some marked negative anomalies for the late RWP period, namely AD 90 and 250 (Fig. 3).

The combined effect of high precipitation and changes in land use (e.g., deforestation and farming, associated with the mining exploitation, intensified soil erosion) carried out by Romans in NW Iberia, and more specifically in the Minho river catchment area, led to a higher loading of terrestrial-derived sediments transported to the shelf by the rivers. A significant increase in river borne detrital material in sediments to the W Iberian shelf is broadly recognized during the RWP (e.g., Lebreiro et al., 2006: 50 BC; Bernárdez et al., 2008a; Bernárdez et al., 2008b: 50 BC–AD 250; Abrantes et al., 2005; Rodrigues et al., 2009; Mohamed et al., 2010: AD 0–550). Foraminiferal data suggests increased fluvial influence at AD 230–280 as indicated by low-salinity species (*T. salsa/irregularis* and *M. fusca*) and the low density. This contrasts with a previous study devoted to the identification of OM sources by using lipid biomarker analysis (de la Rosa et al., 2012) performed at the same location that pointed to an increase contribution of marine

phytoplankton to the organic pool at that time. This disagreement can be explained by the complex processes that control salt marsh settings. For instance, while increase river flow might provide the ecological framework, more frequent or intense storms (recorded between AD 50–300; Behre, 2007) could deposit marine phytoplankton, leaving a geochemical signal but without modifying the brackish conditions. Overwash deposits found at AD 180–310 40 km south of the Minho estuary (Granja, 1999) support this hypothesis.

The uppermost FAZ VI (AD 1080 to 1380) is coeval with the later part of the MCA and the transition to the LIA. The new climatic conditions are reflected in the core sediments in four episodes of very low abundance and poorly preserved foraminifera. The first occurrence at AD 1140 is coeval with a maximum in carbon isotopic composition ($\delta^{13}\text{C}$; De la Rosa et al., 2012; Appendix D) and organic carbon to total nitrogen ratio ($\text{C}_{\text{org}}/\text{N}$), indicating a major input from terrestrial plants at AD 1140–1160 (Appendix D). This is further supported by the lipid content, average chain length of *n*-alkanes (ACL) and terrigenous/aquatic ratio of *n*-alkanes (TAR) values that also suggest an increase in the continental discharges at that time, which is contemporary with major river flood events reported for the same period in this area (De la Rosa et al., 2012). This event could be related with the Oört Solar Minimum (AD 1040–1080), if the date uncertainties are considered. The following episodes occurred at AD 1270, AD 1310 and AD 1340 (Fig. 3), might be related to the Wolf Solar Minimum (AD 1280–1350). Historical records of the 12th and 13th centuries confirm that the Atlantic Iberian region experienced severe winter floods in the years of AD 1102, 1168, 1178, 1181, 1201, 1203, 1207, 1258, 1264

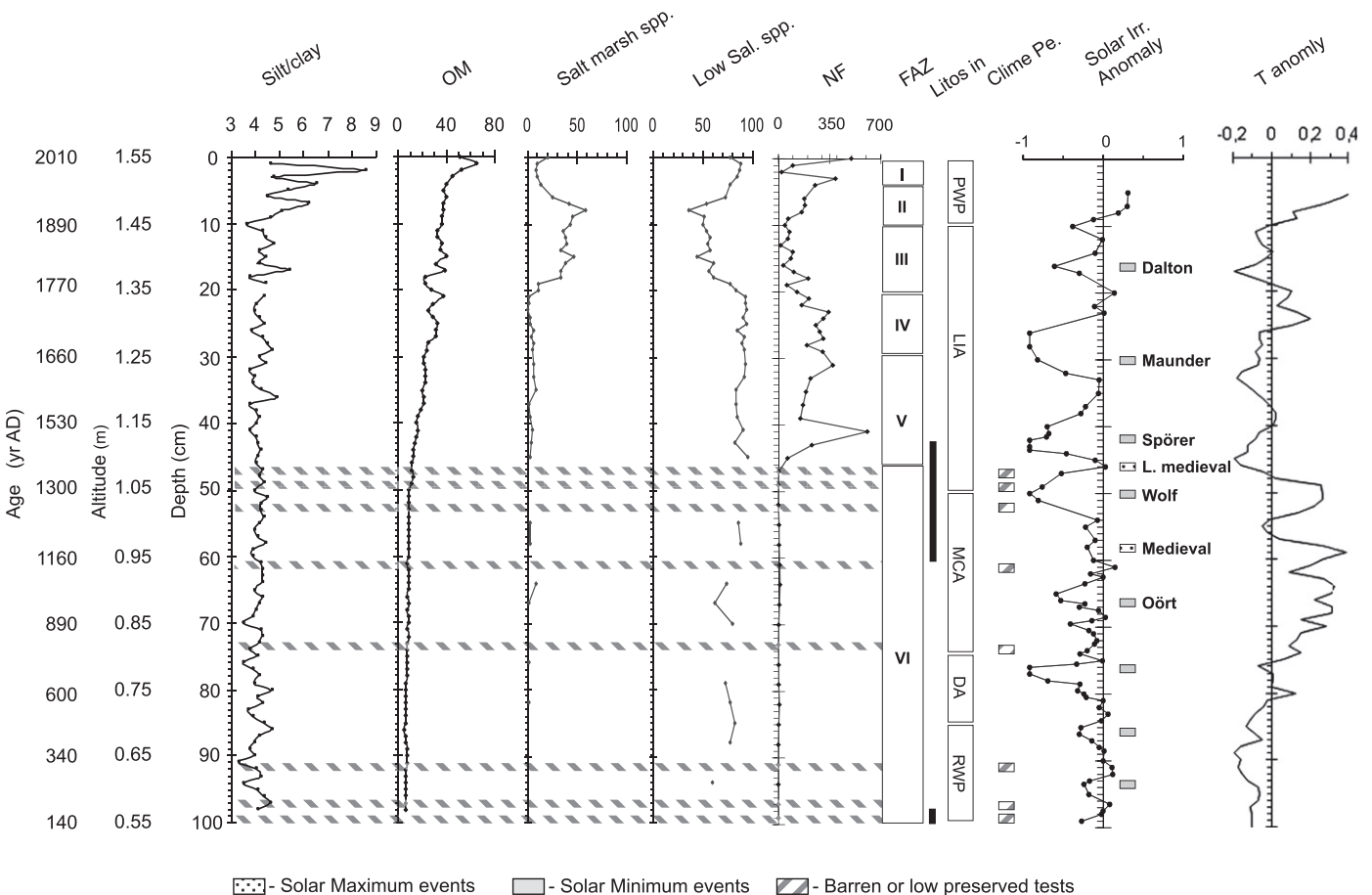


Figure 4. Sedimentological, geochemical and summary of benthic foraminifera data in core FCPw 1. Age (yr AD) – age in calendar years AD; Salt marsh spp. – percentage distributions of the group of brackish salt marsh benthic species; Low Sal. spp. – percentage distributions of the group of low-salinity benthic species; NF – number of foraminifera per cm^2 ; FAZ – foraminiferal assemblage zones; Litos in – periods of continental litogenic inputs to the shelf (see references in the text and Appendix E); Clime Pe. – climate periods in the last 2 milenia (see references in the text); Solar Irr. Anomaly – solar irradiance anomaly using a 22-yr running average reconstruction (after Steinhilber et al., 2012); T anomal. – temperature anomaly using a 10-yr running average reconstruction (after Martín-Chivelet et al., 2011).

and 1310 (Font, 1988; Benito et al., 2008). Sediment cores from the shelf Douro Mud Patch allowed the recognition of abnormal precipitation events resulting in fluvial flooding recorded at AD 1100–1200, coeval with well-marked sea-surface temperature (SST) decreases, shifts in solar activity and more persistent NAO negative phases (Abrantes et al., 2011). Low-salinity foraminiferal assemblages are only well preserved between AD 1190 and 1230, in a period that corresponds to the Medieval Solar Maximum (AD 1100–1250).

In summary, FAZ VI records a prevailing fluvial contribution, leading to a low-salinity environment in spite of the proximity to the river mouth (ca. 3.5 km). If stronger marine input existed, namely at RWP and MCA, it did not last long enough in order to change the environmental conditions of the tidal flats in this sector of the estuary.

Above the tidal flat represented by FAZ VI, a tidal marsh develops (FAZ V) still under low-salinity conditions from AD 1380 to 1690, where foraminiferal assemblages exhibit low diversity but significantly higher density. This suggests that sedimentation rates are large enough to gain elevation in relation to the tidal frame. Salt marsh species *T. comprimata* tends to increase towards the top of this section (36–29 cm depth) after AD 1610 (4–6%; Fig. 3), suggesting that the low marsh environment was already installed, growing from the lower IIB zone (between MtL and MHWN) to IIA zone (between MHWN and MHW) and marking the increase of the marsh palaeoelevation. This important step in Caminha marsh evolution was accompanied by a significant increase in OM and Br content followed by the opposite trend in Zr concentration (Fig. 4; Appendix C). Positive correlations between Br and OM contents in soils and marine sediments were documented at least since the 1970s (e.g., Yamada, 1968; Price et al., 1970). More recent studies have shown that Br cycling in marine and terrestrial ecosystems is strongly influenced by OM (e.g., Leri et al., 2010; Leri and Myneni, 2012). According to these authors the relative ease of natural Br oxidation seems to promote its biogeochemical transformation from inorganic to organic forms, conducting to the incorporation into OM through enzymatic processes related to plant litter decay. Salt marshes are areas of high primary productivity and OM accumulation, thus presenting relatively high amounts of Br, supplied by seawater inundation, in both sediment and flora (Rhew et al., 2002). Considered together, the density of foraminiferal assemblages, the OM and Br data suggest the development of a vegetated low marsh. The up-core lowering of Zr content, observed from the base of FAZ V (Appendix C), provides another evidence of an energy drop caused by the development of vegetation on the marsh surface and consequent flat energy gradients. In fact, heavy minerals like zircon require strong hydrodynamic forces for mobilization and transport and serve as a geochemical proxy of depositional energy (e.g., Dellwig et al., 2000; Kolditz et al., 2012). The accumulation of plant debris and particulate OM, following the development of the low marsh, directly contributes to the increase in sediment coarse particles, preventing the use of silt/clay ratio as a runoff proxy after AD 1380. Geochemical data also record the more depleted values of $\delta^{13}\text{C}$ accompanied by high $\text{C}_{\text{org}}/\text{N}$ ratios, suggesting that a maximum of terrestrial contribution and lipid biomarkers ($\text{C}_{31}/\text{C}_{27\text{al}}$, CPI^{ole} and ACL_{al}) indicate that grass vegetation prevails (De la Rosa et al., 2012; Appendix D) during this FAZ.

After the former phase of uncovered tidal flat conditions, FAZ V marks an important step with the onset of a vegetated low marsh surface after AD 1380, despite the persistent high rainfall, fluvial runoff and intense floods recorded during the LIA (e.g., Benito, 2006; Benito et al., 2008; Bernárdez et al., 2008a; Burdloff et al., 2008; Abrantes et al., 2011; González-Álvarez, 2013; Appendix E). Halophytic plants buffer the energy in the system trapping sediment, which increases the marsh vertical elevation. However, other factors such as deforestation, agriculture and mining play a significant role in sedimentation rates. These factors were exacerbated since the Roman times, which associated with low energetic conditions, lead to the siltation of tide-dominated estuaries (Poirier et al., 2011). This filling up of the Portuguese coastal systems has been reported in many other locations,

namely in Caminha at AD 1541, 1575 and 1582 (Granja, 1990, 2007; Granja and Carvalho, 1992). For instance, in the Royal Courts of Évora (AD 1436), the ship-owners from Viana do Castelo, Ponte de Lima and Vila do Conde stated that they were already silted, preventing the access of larger ships. In fact, the forests depletion in northern Portuguese hinterland attained a critical point that necessitated the import of timber from the north of Spain, France, England and Flanders in order to supply the growing shipbuilding industry (Devy-Vareta, 1986). This was also a period of increased formation of transgressive dune fields. A generalized phase of intense aeolian activity is also distinguished along the Portuguese coast, marked by dune development and enhancement of westerly winds and storminess throughout the LIA, compatible with prolonged negative phases of the NAO (e.g., Clarke and Rendell, 2006; Clemmensen et al., 2009; Costas et al., 2012).

The transition between FAZ V and FAZ IV is marked by the species *T. comprimata* and *P. ipohalina* (AD 1690–1730) and *J. macrescens*, *H. wilberti*, *P. limnetis* and *T. inflata* at the top of FAZ IV (AD 1770). This distribution suggests a gradual evolution from low marsh zone IIA to high marsh zone IB (between MHW and MHWS). It still portrays a markedly low-salinity environment, but the presence (even in low percentage) of these salt marsh species suggests increasing salinity in the area, that might be related to sea-level changes.

The transition from low to high marsh occurs mostly during the Maunder Solar Minimum (AD 1645–1715). The grain size and OM content is still increasing in this FAZ, Br presents its highest content and foraminiferal density remains high, probably reflecting a denser marsh plant cover. During this period, there was a wet phase recorded in Galician continental vegetation (Schellekens et al., 2011), concomitant with the coldest phase of the LIA in Europe that peaked around AD 1700 (e.g., Desprat et al., 2003; Lockwood, 2012; Lockwood et al., 2010; Luterbacher et al., 2001).

FAZ III to I also correspond to a high marsh depositional environment, recording frequent increments of salt marsh species and low foraminiferal density episodes, under general conditions of low salinity. Such variability of assemblages is associated with the end of the LIA and beginning of the PWP, characterized by alternating wet and dry years, namely dryer winter conditions (e.g., Marques, 2001; Abrantes et al., 2011). This reduced river discharge leads to an increase in the marine influence inside the estuary. The beginning of meteorological instrumental record in the NW of Portugal in AD 1864 (FAZ III) allows a better interpretation of proxy data.

The high marsh (foraminiferal IB zone) recorded at FAZ III, is mostly represented by low-salinity assemblages. The species associated with salt marshes are meaningful but with lower percents: *J. macrescens* (12–23%), *T. inflata* (3–22%) and *T. comprimata* (3–13%). The assemblages still have low diversity and density exhibits a significant drop for most of FAZ III (Table 2). The lower density levels, 59 tests/cm³ (AD 1780) and 34 tests/cm³ (AD 1820), tend to be associated with the Dalton Solar Minimum (AD 1790–1820) transitions. Other low values are recorded throughout this event: 17 tests/cm³ (AD 1850) and 44 tests/cm³ (AD 1890). This disparate record between 17 and 205 test/cm³ suggests a biotic response to more stressful conditions, induced by alternating periods of intense rainfall/floods and droughts. In fact, it was a time of major river floods in northern Portugal, as recorded at Douro basin (e.g., Rodrigues et al., 2003; Araújo, 2005). The record of floods from the Atlantic Iberian rivers (south basins included) also suggests higher flood intensification during the periods AD 1730–1760, AD 1780–1810 and AD 1870–1900 (Marques, 2001; Rodrigues et al., 2003; Benito et al., 2008; Appendix E). This alternating climatic pattern switches the system from essentially fluvial controlled to more marine, with increasing salinity in the high marsh ecosystem as a result of higher evaporation rates and higher inputs of marine water into the estuary.

Alternations in the C/N and $\delta^{13}\text{C}$ values through the 18th and 19th centuries were consistent with fluctuations in the *n*-alkyl parameters. These proxies also document regular intensive rainfall alternating

with severe droughts (De la Rosa et al., 2012). Events like storms, cold persistent rains, wet and cool summers, and droughts that caused wine harvest delays, crop loss and famines, high prices of cereals, and plagues are documented for the Minho region throughout the 18th century and the beginning of the 19th century, as well as religious services *pro-pluvia* and *pro-serenitate* (Marques, 2001). These historical records therefore corroborate the climatic pattern suggested by geochemical and foraminiferal proxies.

The lowest foraminifera density level recorded in FAZ II (68 tests/cm³) occurs at AD 1900, probably linked to the solar minimum of AD 1900–1920 (Scaffeta, 2012). Major flooding events of the NW Portuguese main rivers are recorded in the transition from the 19th to the 20th century, like in the Douro (e.g., Rodrigues et al., 2003; Araújo, 2005; Appendix E) and Lima basins: the higher mark of the 20th century Lima river flood, from 1909, may be directly observed on the medieval tower wall of Ponte de Lima.

The analysis of the drought events, based on standardized precipitation index (SPI₁₂ month) for the series of Porto meteorological stations data (1922–2005), reveals that droughts begun in the mid-1930s, attaining their most significant expression (severe to extreme droughts: SPI ≤ −1.5) in the 1940s and 1950s (1944/45, 1949, 1953/54 and 1957; Domingos, 2006). Moreira et al. (2012) noted the same severe and extreme droughts until 1956, followed by a period of decrease in drought episodes. Besides its severity, the Palmer Drought Severity Index (PDSI) notes that the duration of these droughts was the most striking of the instrumental record: 1933–1935, 26 months; 1943–1946, 36 months and 1953–1955, 25 months (Pires et al., 2010). The salt marsh species acme (AD 1934) may therefore be the corollary of these dryer conditions (Fig. 5), probably associated with the solar maximum of AD 1940–1950 (Scaffeta, 2012). After AD 1960, the foraminiferal assemblages gradually become dominated by low-salinity species (>70%) until AD 1983, during the solar minimum AD 1960–1980. This transition points towards a higher fluvial influence in the lower estuary. In fact, the instrumental precipitation recorded in the Minho region (available since 1934; <http://snirh.pt>) shows persistent positive anomalies from 1955 to 1983 (Fatela et al., 2013) and the SPI₁₂ of Porto exhibits the lowest drought indices (Fig. 5). Besides the direct effect of this high precipitation, the river flow and seepage inputs are also enhanced over the high marsh zone, creating ecological conditions that lead to a major presence of low-salinity species.

The enhanced Br concentration shows a direct relation with OM contents throughout this FAZ (10–4 cm depth; AD 1900 to 1985) with higher values at 4–5 cm depth, AD 1983 (Appendix C). The organic geochemical results obtained by De la Rosa et al. (2012) showed a decrease in the terrestrial OM component and an increase of plankton-derived lipid contribution at AD 1960–1985. This was interpreted as a possible enhancement of marine input probably associated with a reduction in the Minho River discharge due to the construction of many major dams or with diagenetic processes induced by the selective degradation of different minerals in sediments affecting, for instance, the C_{org}/N. While the presence of dams might reduce the relationship between precipitation and runoff, the good correlation between these two parameters (DeCastro et al., 2006; Gómez-Gesteira et al., 2011; Fatela et al., 2013) suggests that this is not the case here. Also, it should be noted that the intense dredging in the Minho lower estuary, mainly between 1960 and 1990 (Alves, 1996; Delgado, 2011), caused an intense remobilization of sediments. The process of sand extraction also included the wash of these materials leaving the mud fraction (OM included) inside the estuary during rising tides. These anthropic activities likely promoted remobilization, transport and redeposition of the mud fraction, contributing to the intensification of the geochemical marine signal in the tidal marshes. The foraminiferal assemblages highlight that rainfall increased the brackish ecological conditions at the high marsh, in spite of the enhanced marine geochemical records for this time.

Increase fluvial influence is also recorded in FAZ I by the OM proxies (De la Rosa et al., 2012). Foraminiferal assemblages are consistent

with the present-day high marsh zone IB. This assemblage reflects the modern hydroclimatic balance in the Minho lower estuary, where low-salinity species prevail at higher high marsh zones (Fig. 3; Table 2), mostly under brackish/fresh estuarine water. The lowest values of foraminiferal density reflect the precipitation positive anomalies and the intensification of flood events (Fatela et al., 2013).

Brackish conditions have persisted in the Minho estuary at least since 140 AD. The intertidal sedimentary record highlights two main steps – tidal flat and marsh – where the preservation of proxies information, namely benthic foraminifera, is quite distinct. The tidal flat assemblages are poorly preserved and often absent, in this environment where the hydrogeochemical pattern is marked by a general baseline depleted in calcium carbonate (Moreno et al., 2007; Valente et al., 2009). Even so, it is clear that the residual assemblages are predominantly composed by low-salinity species. The sediment accretion leads to the marsh installation after AD 1380 and the development of a plant cover that reduces hydrodynamics energy, acts as a sediment trap and improves the assemblages' preservation. Marsh foraminiferal response firstly reflects the elevation change from tidal flat to high marsh and the hydrological balance inside the estuary.

The hydrological balance is closely connected to climate variability during the last millennia and its dependant on the fluctuations in solar activity (e.g., Duhau, 2006; Jager and Duhau, 2009; Jager and Nieuwenhuijzen, 2013; Keller, 2004; Lean, 2010; Mörner, 2010; Shindell et al., 2001; Usoskin, 2013; Versteegh, 2005; Wanner et al., 2008), which drives the position, migration and stability of atmospheric systems (e.g., Haigh, 2007) and oceanic circulation (e.g., Mörner, 2010). According to Shindell et al. (2001) and Martín-Puertas et al. (2012), the modeling of climate response to periods of low solar activity coupled with low NAO index and led to a southward displacement of the westerlies. Therefore, as a response to reduced solar activity, European mid-latitudes experienced colder temperatures and increased humidity. The palaeoclimatic records of the Iberian Peninsula continental shelf reveal increased river discharge during periods of NAO-negative (Álvarez et al., 2005; Lebreiro et al., 2006; Bernárdez et al., 2008b; Abrantes et al., 2011; González-Álvarez, 2013) and the instrumental data show good correlations between negative phases of NAO index and winter precipitation and river flow in NW Iberia, namely in Minho river basin (e.g., Trigo et al., 2004; DeCastro et al., 2006; Fatela et al., 2013). The hydrological balance recorded by the Caminha marsh foraminifera and sedimentological proxies is controlled by the atmospheric modes, reflecting the NE Atlantic climate dynamic, namely from LIA to present.

Conclusions

Foraminiferal assemblages reveal the palaeoenvironmental evolution of NW Portugal estuaries, primarily in the intertidal zone. The assemblages, associated with sedimentological and geochemical proxies, provided a detailed reconstruction for the last two millennia. Six Foraminiferal Assemblage Zones (FAZ) have been considered in this period. The tidal flat environment prevailed in the riverbanks of Minho low estuary until the end of the 14th century, when vertical accretion led to the colonization by halophyte plants and the development of a stable low marsh environment. The natural continuity of this process, probably enhanced by anthropogenic activities, resulted in the establishment of the high marsh zone, beginning at about the 18th century. Foraminiferal species and the density of their assemblages revealed to be a fundamental tool to the recognition of the estuarine hydrological balance, namely between predominantly marine or fluvial conditions as result of wet or dry periods. Estuarine evolution mainly occurred under brackish conditions reflected by the dominance of low-salinity species, where the flood events created a drop in the foraminiferal density. The drought periods are marked by an increase in the proportion of salt marsh species that dominated the assemblages during the most severe events recorded in the middle of 20th century. The stronger influence of

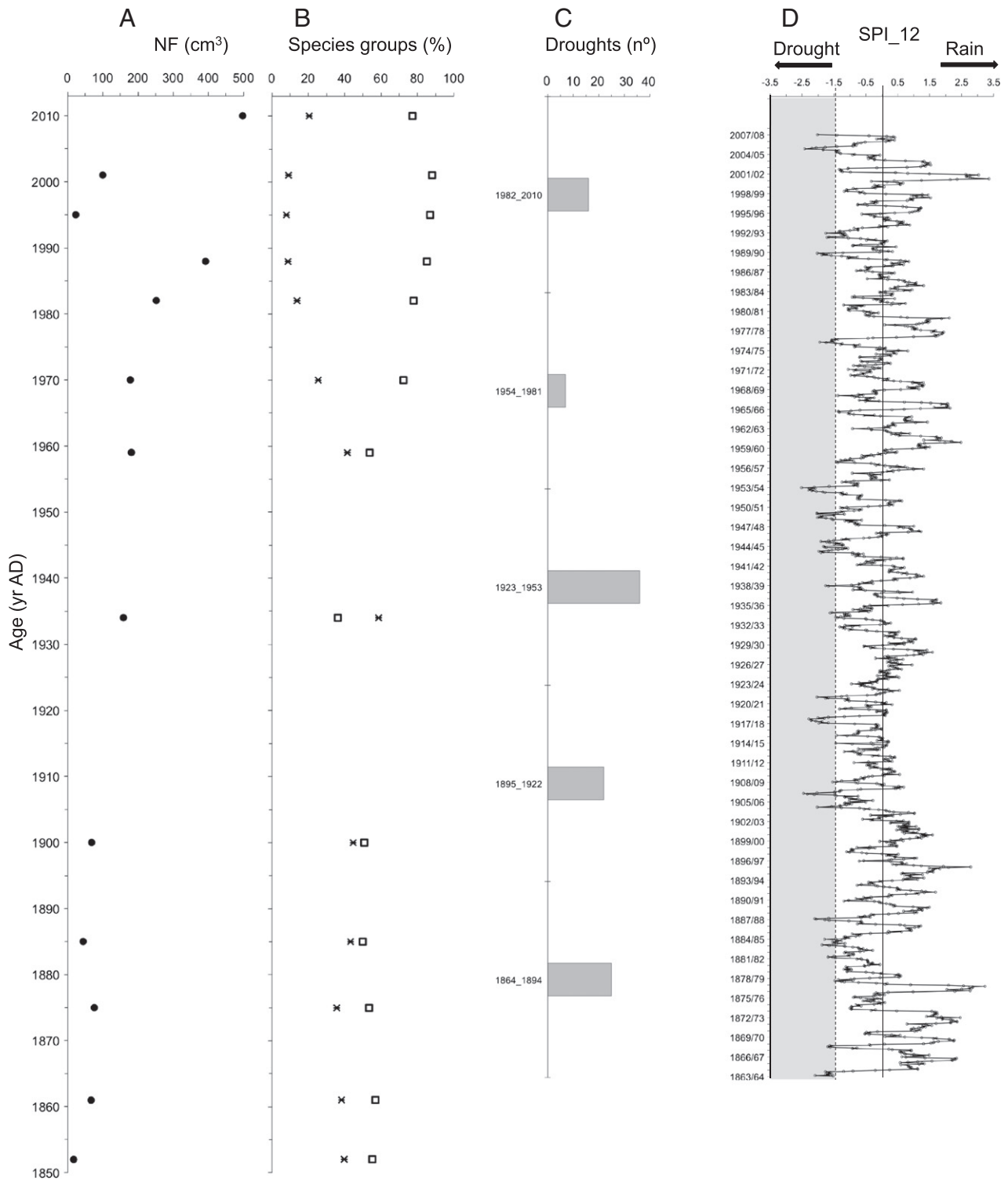


Figure 5. Relationship between foraminiferal data and Standardized Precipitation Index (12 months: SPI₁₂, after Moreira et al. (2012)), from Porto (Serra do Pilar: 41° 08' 19.20" N–08° 36' 09.68" W). A – number of foraminifera per cm³; B – percentage of “normal” (stars) and “low” salinity (open squares) species; C – number of severe and extreme droughts (gray bars) calculated with the SPI₁₂, grouped in intervals of ca. 30 yr, from 1864 to 1894, 1895 to 1922, 1923 to 1953 and 1982 to 2010; D – SPI₁₂ time series, from hydrological year 1863/64 to 2007/08), gray column represents the field of severe and extreme droughts (SPI ≤ –1.5).

marine or fluvial conditions inside the estuary over RWP, MCA, LIA and PWP appears closely connected to climate variability (in dependence upon the fluctuations in solar activity), highlighting the contribution of marsh foraminifera from SW Europe to the understanding of NE Atlantic regional climate evolution.

Acknowledgments

This work is a contribution of the WestLog (PTDC/CTE/105370/2008) project, funded by the Fundação para a Ciência e Tecnologia – FCT, that includes the grants of João Moreno, Inês Pereira and Ana Medeiros. Jose

de la Rosa's participation was funded through the Ciência 2008 framework (FCT) at IST/CTN. It is also a contribution to the IGCP Project 588, Northwest Europe working group of the INQUA Commission on Coastal and Marine Processes and the Geo-Q Zentroa Research Unit (Joaquín Gómez de Llarena Laboratory), Sociedad de Ciencias Aranzadi.

We are grateful to Elsa Moreira (Centro de Matemática e Aplicações, Faculdade de Ciências e Tecnologia – UNL) who kindly provided SPI data series from Porto. We also thank Peter Langdon, Derek Booth and two anonymous reviewers for their comments that improved the final manuscript.

Appendix A. Supplementary data

Supplementary data to this article can be found online at <http://dx.doi.org/10.1016/j.yqres.2014.04.014>.

References

- Abrantes, F., Lebreiro, S., Rodrigues, T., Gil, I., Bartels-Jónsdóttir, H., Oliveira, P., Kissel, C., Grimalt, J.O., 2005. Shallow marine sediment cores record climate variability and earthquake activity off Lisbon (Portugal) for the last 2,000 years. *Quaternary Science Reviews* 24, 2477–2494.
- Abrantes, F., Rodrigues, T., Montanari, B., Santos, C., Witt, L., Lopes, C., Voelker, A.H.L., 2011. Climate of the last millennium at the southern pole of the North Atlantic Oscillation: an inner-shelf sediment record of flooding and upwelling. *Climate Research* 48, 261–280.
- Alday, M., Cearreta, A., Cachão, M., Freitas, M.C., Andrade, C., Gama, C., 2006. Micropaleontological record of Holocene estuarine and marine stages in the Corgo do Porto rivulet (Mira River, SW Portugal). *Estuarine, Coastal and Shelf Science* 66, 532–543.
- Álvarez, M., Flores, J., Sierro, F., Diz, P., Francés, G., Pelejero, C., Grimalt, J., 2005. Millennial surface water dynamics in the Ria de Vigo during the last 3000 years as revealed by coccoliths and molecular biomarkers. *Palaogeography, Palaeoclimatology, Palaeoecology* 218, 1–13.
- Alves, A., 1996. Causas e Processos da Dinâmica Sedimentar na Evolução Actual do Litoral do Alto Minho. Unpublished PhD thesis, Universidade do Minho, Braga, Portugal. 442 pp.
- Andersen, H.V., 1953. Two new species of *Haplophragmoides* from the Louisiana coast. Contributions from the Cushman Foundation for Foraminiferal Research 4, 21–22.
- Appleby, P.G., Oldfield, F., 1992. Application of ^{210}Pb to sedimentation studies. In: Ivanovich, M., Harmon, R.S. (Eds.), *Uranium Series Disequilibrium*. Oxford University Press, Oxford, pp. 731–778.
- Araújo, E.L.S., 2005. Geoturismo: Conceptualização, Implementação e Exemplo de Aplicação ao Vale do Rio Douro no Sector Porto-Pinhão. Unpublished MSc thesis, Universidade do Minho, Braga, 213 pp.
- Araújo, M.F., Valério, P., Jouanneau, J.-M., 1998. Heavy metal assessment in sediments of the Ave river basin (Portugal) by EDXRF. *X-Ray Spectrometry* 27, 305–312.
- Araújo, M.F., Conceição, A., Barbosa, T., Lopes, M.T., Humanes, H., 2003. Elemental composition of marine sponges from the Berlengas natural park, western Portuguese coast. *X-Ray Spectrometry* 32, 428–433.
- Behre, K.-E., 2007. A new Holocene sea-level curve for the southern North Sea. *Boreas* 36, 82–102 (January).
- Benito, G., 2006. Paleofloods and historical flood records along the middle Tagus river catchment: climatic and flood hazard implications. *Tagus Floods Abstracts* p. 35.
- Benito, G., Machado, M.J., Pérez-González, A., 1996. Climate change and flood sensitivity in Spain. In: Branson, J., Brown, A.G., Gregory, K.J. (Eds.), *Global Continental Changes: The Context of Palaeohydrology*. Geological Society Special Publication, 115, pp. 95–98.
- Benito, G., Thornycraft, V.R., Rico, M., Sánchez-Moya, Y., Sopena, A., 2008. Palaeoflood and floodplain records from Spain: evidence for long-term climate variability and environmental changes. *Geomorphology* 101, 68–77.
- Benito, G., Rico, M., Sánchez-Moya, Y., Sopena, A., Thornycraft, V.R., Barriendos, M., 2010. The impact of late Holocene climatic variability and land use change on the flood hydrology of the Guadalentín River, southeast Spain. *Global and Planetary Change* 70, 53–63.
- Bernárdez, P., González-Álvarez, R., Francés, G., Prego, R., Bárcena, M.A., Romero, O.E., 2008a. Late Holocene history of the rainfall in the NW Iberian peninsula – evidence from a marine record. *Journal of Marine Systems* 72, 366–382.
- Bernárdez, P., González-Álvarez, R., Francés, G., Prego, R., Bárcena, M.A., Romero, O.E., 2008b. Palaeoproductivity changes and upwelling variability in the Galicia Mud Patch during the last 5000 years: geochemical and microfloral evidence. *The Holocene* 18, 1207–1218.
- Bettencourt, A., Ramos, L., Gomes, V., Dias, J.M.A., Ferreira, G., Silva, M., Costa, L., 2003. In: INAG (Ed.), *Estuários Portugueses*. Ministério das Cidades, Ordenamento do Território e Ambiente, Lisboa (311 pp.).
- Bradley, R.S., Jones, P.D., 1993. 'Little Ice Age' summer temperature variations: their nature and relevance to recent global warming trends. *The Holocene* 3, 367–376.
- Brady, H.B., 1870. Analysis and descriptions of the Foraminifera. *Annals and Magazine of Natural History* 4 (6), 273–309.
- Brönnimann, P., 1986. *Paratrochammina* (Lepidoparatrochammina) guaratibaensis n. sp. from Brackish Waters of Brazil and a Check List of Recent Trochamminaceans from Brackish Waters (Protista : Foraminiferida). *Revue Paléobiologie* 5, 221–229.
- Brown, J., Colling, A., Park, D., Philips, J., Rothery, D., Wright, J., 1991. *Waves, Tides and Shallow-water Processes*. The Open University (187 pp.).
- Burdloff, D., Araújo, M.F., Jouanneau, J.-M., Mendes, I., Monge Soares, A.M., Dias, J.M.A., 2008. Sources of organic carbon in the Portuguese continental shelf sediments during the Holocene period. *Applied Geochemistry* 23, 2857–2870.
- Clarke, M.L., Rendell, H.M., 2006. Effects of storminess, sand supply and the North Atlantic Oscillation on sand invasion and coastal dune accretion in western Portugal. *The Holocene* 16, 341–355.
- Clemmensen, L.B., Murray, A., Heinemeier, J., de Jong, R., 2009. The evolution of Holocene coastal dune fields, Jutland, Denmark: a record of climate change over the past 5000 years. *Geomorphology* 105, 303–313.
- Cook, E.R., Seager, R., Heim Jr., R.R., Vose, R.S., Herweijer, C., Woodhouse, C., 2010. Megadroughts in North America: placing IPCC projections of hydroclimatic change in a long-term palaeoclimate context. *Journal of Quaternary Science* 25, 48–61.
- Costas, S., Jerez, S., Trigo, R.M., Goble, R., Rebêlo, L., 2012. Sand invasion along the Portuguese coast forced by westerly shifts during cold climate events. *Quaternary Science Reviews* 42, 15–28.
- Cushman, J.A., Bronnimann, P., 1948. Some new genera and species of foraminifera from brackish water of Trinidad. *Contributions from the Cushman Laboratory for Foraminiferal Research* 24, 15–21.
- De la Rosa, J.M., Araújo, M.F., González-Pérez, J.A., González-Vila, F.J., Soares, A.M., Martins, J.M., Leorri, E., Corbett, R., Fatela, F., 2012. Organic matter sources for tidal marsh sediment over the past two millennia in the Minho River estuary (NW Iberian Peninsula). *Organic Geochemistry* 53, 16–24.
- Debenay, J.-P., Guiral, D., Parra, M., 2002. Ecological factors acting on microfauna in mangrove swamps. The case of foraminiferal assemblages in French Guiana. *Estuarine, Coastal and Shelf Science* 55, 509–533.
- DeCastro, M., Lorenzo, M., Taboada, J.J., Sarmiento, M., Alvarez, I., Gómez-Gesteira, M., 2006. Influence of teleconnection patterns of precipitation variability and on river flow regimes in the Miño River basin (NW Iberian Peninsula). *Climate Research* 32, 63–73.
- Delgado, A., 2011. Caracterização hidrográfica e sedimentar do estuário do rio Minho. Unpublished MSc thesis, Universidade do Porto, Portugal. 197 pp.
- Dellwig, O., Hinrichs, J., Hild, A., Brumsack, H.-J., 2000. Changing sedimentation in tidal flat sediments of the southern North Sea from the Holocene to the present: a geochemical approach. *Journal of Sea Research* 44, 195–208.
- Desprat, S., Goñi, M.F.S., Loutre, M.-F., 2003. Revealing climatic variability of the last three millennia in northwestern Iberia using pollen influx data. *Earth and Planetary Science Letters* 213, 63–78.
- Devy-Vareta, N., 1986. Para uma geografia histórica da floresta portuguesa. do declínio das matas medievas à política florestal do renascimento (séc. xv e xvi). *Revista da Faculdade de Letras – Geografia. I Série, vol. I. Porto*, pp. 5–37.
- Domingos, S.I.S., 2006. Análise do índice de seca Standardized Precipitation Index (SPI) em Portugal Continental e sua comparação com o Palmer Drought Severity Index (PDSI). Unpublished Msc thesis, Universidade de Lisboa, Portugal, 53 pp.
- Dominguez-Castro, F., Santisteban, J.L., Barriendos, M., Mediavilla, R., 2008. Reconstruction of drought episodes for central Spain from roganation ceremonies recorded at Toledo Cathedral from 1506 to 1900: a methodological approach. *Global and Planetary Change* 63, 230–242.
- Do Ó, A., Roxo, M.J., 2008. Drought events in Southern Portugal from the 12th to the 19th centuries: integrated research from descriptive sources. *Natural Hazards* 47, 55–63.
- Drago, T., Freitas, M.C., Rocha, F., Cachão, M., Moreno, J., Naughton, F., Fradique, C., Araújo, F., Silveira, T., Oliveira, A., Cascalho, J., Fatela, F., 2006. Paleoenvironmental evolution of estuarine systems during the last 14 000 years – the case of Douro estuary (NW Portugal). *Journal of Coastal Research*, SI 39, 186–192.
- Duhau, S., 2006. Solar activity, Earth's rotation rate and climate variations in the secular and semi-secular time scales. *Physics and Chemistry of the Earth* 31, 99–108.
- Fatela, F., Taborada, R., 2002. Confidence limits of species proportions in microfossil assemblages. *Marine Micropaleontology* 45, 169–174.
- Fatela, F., Moreno, J., Antunes, C., 2007. Salinity influence on foraminiferal tidal marsh assemblages of NW Portugal: an anthropogenic constraint? *Thalassas, An International Journal of Marine Sciences* 23, 51–63.
- Fatela, F., Moreno, J., Moreno, F., Araújo, M.F., Valente, T., Antunes, C., Taborada, R., Andrade, C., Drago, T., 2009. Environmental constraints of foraminiferal assemblages distribution across a brackish tidal marsh (Caminha, NW Portugal). *Marine Micropaleontology* 70, 70–88.
- Fatela, F., Moreno, J., Leorri, E., Corbett, R., 2013. High marsh foraminiferal assemblages response to intra-decadal and multi-decadal precipitation variability, between 1934 and 2010 (Minho, NW Portugal). *Journal of Sea Research*. <http://dx.doi.org/10.1016/j.seares.2013.07.021>.
- Font, Tullot I., 1988. *Historia del clima de España*. Spanish Meteorological Institute (INM), Madrid (297 pp.).
- Gehrels, W.R., 1994. Determining relative sea level change from salt marsh foraminifera and plant zones on the coast of Maine, USA. *Journal of Coastal Research* 10, 990–1009.
- Gehrels, W.R., Newman, S.W.G., 2004. Salt-marsh foraminifera in Ho Bugt, western Denmark, and their use as sea-level indicators. *Danish Journal of Geography* 104, 49–58.
- Gil-García, M.J., Ruiz Zapata, M.B., Mediavilla, R., Santisteban, J.L., Dominguez-Castro, F., Dabrio, C.J., 2008. Registro de los cambios humanos y naturales en el humedal de las Tablas de Daimiel (Ciudad Real, España). *Geo-Temas* 10, 1471–1474.
- Gómez-Gesteira, M., Gimeno, L., de Castro, M., Lorenzo, M.N., 2011. The state of climate in NW Iberia. *Climate Research* 48, 109–144.
- González-Álvarez, R., 2013. Cambios climáticos de pequeña magnitud durante el Holoceno: sus efectos en la paleoceanografía de la plataforma continental gallega. Unpublished PhD thesis, Universidade de Vigo, España, 306 pp.
- Graham, N.E., Ammann, C.M., Fleitmann, D., Cobb, K.M., Luterbacher, J., 2011. Support for global climate reorganization during the “medieval climate anomaly”. *Climate Dynamics* 37, 1217–1245. <http://dx.doi.org/10.1007/s00382-010-0914-z>.

- Granja, H.M., 1990. Representar a geodinâmica da zona costeira: o passado e o presente; que futuro? Unpublished PhD Thesis, Universidade do Minho, Braga, Portugal. 347 pp.
- Granja, H.M., Carvalho, G.S., 1992. Dunes and Holocene deposits of the coastal zone of Portugal, north Mondego Cape. In: Carter, R.W.G., Curtis, T.G.F., Sheehy-Skeffington, M.J. (Eds.), *Coastal Dunes: Geomorphology, Ecology and Management for Conservation*. Proceedings of the Third European Dune Congress, Galway, Ireland, pp. 43–50.
- Granja, H.M., 1999. Evidence for Late Pleistocene and Holocene sea-level, neo-tectonic and climatic control in the coastal zone of northwest Portugal. *Geologie en Mijnbouw* 77, 233–245.
- Granja, H.M., 2007. Multidisciplinary analysis of historical sources – The geomorphological approach. European Seaport Systems in the early modern age. A comparative approach. International Workshop Proceedings, Porto, IHM-UP, pp. 70–78.
- Haigh, J.D., 2007. The sun and the earth's climate. *Living Reviews in Solar Physics* 4, 1–64 (URL accessed 03.12.13: <http://www.livingreviews.org/lrsp-2007-2>).
- Haslett, J., Parnell, A., 2008. A simple monotone process with application to radiocarbon-dated depth chronologies. *Applied Statistics* 57, 399–418.
- Hayward, B.W., Grenfell, H.R., Reid, C.M., Hayward, K.A., 1999. Recent New Zealand Shallow-water Benthic Foraminifera: Taxonomy, Ecologic Distribution, Biogeography, and Use in Paleoenvironmental Assessment, Institute of Geological & Nuclear Sciences, Lower Hutt, New Zealand (monograph 21, 264 pp.).
- Head, K., 1980. Manual of soil laboratory testing. Volume 1: Soil Classification and Compaction Tests, Pentech Press, London (339 pp.).
- Hippensteel, S.P., Martin, R.E., Harris, M.-S., 2005. Records of prehistoric hurricanes on the South Carolina coast based on micropaleontological and sedimentological evidence, with comparison to other Atlantic Coast records: discussion. *Geological Society of America Bulletin* 117, 250–253.
- Horton, B.P., 1999. The distribution of contemporary intertidal foraminifera at Cowpen Marsh, Tees Estuary, UK: implications for studies of Holocene sea-level changes. *Palaeogeography, Palaeoclimatology, Palaeoecology* 149, 127–149.
- Horton, B.P., Edwards, R.J., 2005. The application of local and regional transfer functions to the reconstruction of Holocene sea levels, north Norfolk, England. *The Holocene* 15, 216–228.
- Horton, B.P., Murray, J.W., 2006. Patterns in cumulative increase in live and dead species for foraminiferal time series of Cowpen Marsh, Tees Estuary, UK: implications for sea-level studies. *Marine Micropaleontology* 58, 287–315.
- Horton, B.P., Culver, S.J., 2008. Modern intertidal foraminifera of the Outer Banks, North Carolina, U.S.A. and their applicability for sea-level studies. *Journal of Coastal Research* 24, 1110–1125.
- Jager, C., Duhau, S., 2009. Episodes of relative global warming. *Journal of Atmospheric and Solar-Terrestrial Physics* 71, 194–198.
- Jager, C., Nieuwenhuijzen, H., 2013. Terrestrial ground temperature variations in relation to solar magnetic variability, including the present Schwabe cycle. *Natural Science* 5, 1112–1120.
- Keigwin, L.D., Pickart, R.S., 1999. Slope water current over the Laurentian Fan on interannual to millennial time scales. *Science* 286, 520–523.
- Keller, C., 2004. 1000 years of climate change. *Advances in Space Research* 34, 315–322.
- Kolditz, K., Dellwig, O., Barkowski, J., Bahlo, R., Leippe, T., Freund, H., Rgen Brumsack, H.-J., 2012. Geochemistry of Holocene salt marsh and tidal flat sediments on a barrier island in the southern North Sea (Langeoog, North-west Germany). *Sedimentology* 59, 337–355.
- Lamb, H.H., 1985. *Climate History and the Future*, Princeton University Press (835 pp.).
- Lean, J.L., 2010. Cycles and trends in solar irradiance and climate. *WIREs: Climate Change* 1, 111–122. <http://dx.doi.org/10.1002/wcc.018>.
- Lebreiro, S.M., Frances, G., Abrantes, F., Diz, P., Bartels-Jónsdóttir, H.B., Stroynowski, Z.N., Gil, I.M., Pena, L.D., Rodrigues, T., Jones, P.D., Nombela, M.A., Alejo, I., Briffa, K.R., Harris, I., Grimalt, J.O., 2006. Climate change and coastal hydrographic response along the Atlantic Iberian margin (Tagus Prodelta and Muros Ria) during the last two millennia. *The Holocene* 16, 1003–1015.
- Leorri, E., Horton, B.P., Cearreta, A., 2008. Development of a foraminifera-based transfer function in the Basque marshes. *Marine Geology* 251, 60–74.
- Leorri, E., Cearreta, A., 2009a. Quantitative assessment of the salinity gradient within the estuarine systems in the southern Bay of Biscay using benthic foraminifera. *Continental Shelf Research* 29, 1226–1239.
- Leorri, E., Cearreta, A., 2009b. Recent sea-level changes in the southern Bay of Biscay: transfer function reconstructions from salt-marshes compared with instrumental data. *Scientia Marina* 73, 287–296.
- Leorri, E., Gehrels, W.R., Horton, B.P., Fatela, F., Cearreta, A., 2010a. Distribution of foraminifera in salt marshes along the Atlantic coast of SW Europe: tools to reconstruct past sea-level variations. *Quaternary International* 221, 104–115.
- Leorri, E., Cearreta, A., Corbett, R., Blake, W., Fatela, F., Gehrels, R., Irabien, M.J., 2010b. Identification of suitable areas for high-resolution sea-level studies in SW Europe using commonly applied 210Pb models. *Geocata* 48, 35–38.
- Leorri, E., Fatela, F., Cearreta, A., Moreno, J., Antunes, C., Drago, T., 2011. Assessing the performance of a foraminifera-based transfer function to estimate sea-level changes in northern Portugal. *Quaternary Research* 75, 278–287.
- Leorri, E., Drago, T., Fatela, F., Bradley, S., Moreno, J., Cearreta, A., 2013. Late Glacial and Holocene coastal evolution in the Minho estuary (N. Portugal): implications for understanding sea-level changes in Atlantic Iberia. *The Holocene* 23, 352–362.
- Leri, A.C., Myneni, S.C.B., 2012. Natural organobromine in terrestrial ecosystems. *Geochimica et Cosmochimica Acta* 77, 1–10.
- Leri, A.C., Hakala, A., Marcus, M.A., Lanzirrotti, A., Reddy, C.M., Myneni, S.C.D., 2010. Natural organobromine in marine sediments: new evidence of biogeochemical Br cycling. *Global Biogeochemical Cycles* 24 (GB4017), 1–15.
- Llasat, M.-C., Barriendos, M., Barrera, A., Rigo, T., 2005. Floods in Catalonia (NE Spain) since the 14th century. Climatological and meteorological aspects from historical documentary sources and old instrumental records. *Journal of Hydrology* 313, 32–47.
- Lockwood, M., 2012. Solar Influence on Global and Regional Climates. *Surveys in Geophysics* 33, 503–534. <http://dx.doi.org/10.1007/s10712-012-9181-3>.
- Lockwood, M., Harrison, R.G., Woollings, T., Solanki, S.K., 2010. Are cold winters in Europe associated with low solar activity? *Environmental Research Letters* 5 (024001), 1–7. <http://dx.doi.org/10.1088/1748-9326/5/2/024001>.
- Loeblich Jr., A.R., Tappan, H., 1988. *Foraminiferal Genera and their Classification*, v. 1. Van Nostrand Reinhold Company (970 pp., v. 2, 847 pl.).
- Luque, J.A., Juliá, R., 2002. Lake sediment response to land-use and climate change during the last 1000 years in the oligotrophic Lake Sanabria (northwest of Iberian Peninsula). *Sedimentary Geology* 148, 343–355.
- Luterbacher, J., Rickli, R., Xoplaki, E., Tinguely, C., Beck, C., Pfister, C., Wanner, H., 2001. The Late Maunder Minimum (1675–1715) – a key period for studying decadal scale climatic change in Europe. *Climatic Change* 49, 441–462.
- Mann, M.E., Zhang, Z., Rutherford, S., Bradley, R.S., Hughes, M.K., Shindell, D., Ammann, C., Faluvegi, G., Ni, F., 2009. Global signatures and dynamical origins of the little ice age and medieval climate anomaly. *Science* 326, 1256–1260.
- Marques, J., 2001. Estados do Tempo e Outros Fenómenos na Região de Braga, no Século XVII, Vol. I, n. 2. Bracara Augusta, pp. 104–105 (117–118).
- Marquina, J.R., 1949. Crecidas Extraordinarias del Rio Duero. *Revista de Obras Públicas I* (3), 202–213.
- Martín-Chivelet, J., Muñoz-García, M.B., Edwards, R.L., Terrero, M.J., Ortega, A.I., 2011. Land surface temperature changes in Northern Iberia since 4000 yr BP, based on $\delta^{13}C$ of speleothems. *Global and Planetary Change* 77, 1–12.
- Martínez Cortizas, A., Pontevedra-Pombal, X., Garcia-Rodeja, E., Novoa-Muñoz, J.C., Shoyk, W., 1999. Mercury in a Spanish peat bog: archive of climate change and atmospheric metal deposition. *Science* 284, 939–942.
- Martin-Puertas, C., Valero-Garcés, B.L., Mata, M.P., Gonzalez-Samperiz, P., Bao, R., Moreno, A., Stefanova, V., 2008. Arid and humid phases in Southern Spain during the last 4000 years: the Zonar Lake record, Cordoba. *The Holocene* 18, 1–15.
- Martin-Puertas, C., Matthes, K., Brauer, A., Muscheler, R., Hansen, F., Petrick, C., Aldahan, A., Possnert, G., van Geel, B., 2012. Regional atmospheric circulation shifts induced by a grand solar minimum. *Nature Geoscience* 5, 397–401.
- McKee, T.B., Doesken, N.J., Kleist, J., 1993. The relationship of drought frequency and duration to time scales. 8th Conference on Applied Climatology. American Meteorological Society, Boston, pp. 179–184.
- Mohamed, K.J., Rey, D., Rubio, B., Vilas, F., Frederichs, T., 2010. Interplay between detrital and diagenetic processes since the last glacial maximum on the northwest Iberian continental shelf. *Quaternary Research* 73, 507–520.
- Montagu, C., 1808. *Testacea Britannica supplement*, S. Woolmer, Exeter, England (183 pp.).
- Moreira, E.E., Mexia, J.T., Pereira, L.S., 2012. Are drought occurrence and severity aggravating? A study on SPI drought class transitions using log-linear models and ANOVA-like inference. *Hydrological Earth System Sciences* 16, 3011–3028.
- Moreno, F., Araújo, M.F., Moreno, J., Fatela, F., Drago, T., 2005b. Caracterização geoquímica de sedimentos superficiais do estuário do rio Minho e do sapal de Caminha (NW de Portugal) – estimativa do potencial de stress biológico. XIV Semana de Geoquímica & VIII Congresso de Geoquímica dos Países de Língua Portuguesa. Universidade de Aveiro, Portugal, pp. 675–678.
- Moreno, F., Moreno, J., Fatela, F., Valente, T., Guise, L., Araújo, M.F., Drago, T., 2005c. Geoquímica de sedimentos em ambientes típicos de sapal – o exemplo do sapal de Caminha (NW de Portugal). XIV Semana de Geoquímica & VIII Congresso de Geoquímica dos Países de Língua Portuguesa. Univ. Aveiro, Portugal, pp. 661–664.
- Moreno, J., Fatela, F., Andrade, C., Cascalho, J., Moreno, F., Drago, T., 2005a. Living Foraminiferal assemblages from Minho/Coura estuary (Northern Portugal): a stressfull environment. *Thalassas* 21, 17–28.
- Moreno, J., Fatela, F., Andrade, C., Drago, T., 2006. Distribution of “living” Pseudohurammia limnetis (Scott and Mediol) : an occurrence on the brackish tidal marsh of Minho/Coura estuary – Northern Portugal. *Revue de Micropaleontologie* 49, 45–53.
- Moreno, J., Valente, T., Moreno, F., Fatela, F., Guise, L., Patinha, C., 2007. Calcareous foraminifera occurrence and calcite-carbonate equilibrium conditions – a case study in Minho/Coura estuary (N Portugal). *Hydrobiologia* 597, 177–184.
- Mörner, N.-X., 2010. Solar Minima, Earth's rotation and Little Ice Ages in the past and in the future. *The North Atlantic-European case*. *Global and Planetary Change* 72, 282–293.
- Murray, J.W., 1971. *An Atlas of British Recent Foraminiferids*. Heinemann Educational Books (244 pp.).
- Murray, J.W., 2006. *Ecology and Applications of Benthic Foraminifera*. Cambridge University Press, Cambridge (438 pp.).
- Nittrouer, C.A., Sternberg, R.W., Carpenter, R., Bennett, J.T., 1979. The use of ^{210}Pb geochronology as a sedimentological tool: application to the Washington Continental Shelf. *Marine Geology* 31, 297–316.
- Parnell, A., Haslett, J., Allen, J., Buck, C., Huntley, B., 2008. A flexible approach to assessing synchronicity of past events using Bayesian reconstructions of sedimentation history. *Quaternary Science Reviews* 27, 1872–1885.
- Pfister, C., Garnier, E., Alcoforado, M.-J., Wheeler, D., Luterbacher, J., Nunes, M.F., Taborda, J.P., 2010. The meteorological framework and the cultural memory of three severe winter-storms in early eighteenth-century Europe. *Climatic Change* 101, 281–310.
- Phleger, F.B., 1965. Patterns of marsh foraminifera, Galveston Bay, Texas. *Limnology and Oceanography* 10, 169–180.
- Pires, V.C., Álvaro, S., Mendes, L., 2010. Riscos de secas em Portugal continental. *Territorium* 17, 27–34.
- Pla, S., Catalan, J., 2005. Chrysophyte cysts from lake sediments reveal the submillennial winter/spring climate variability in the northwestern Mediterranean region throughout the Holocene. *Climate Dynamics* 24, 263–278.

- Poirier, C., Chaumillon, E., Arnaud, F., 2011. Siltation of river-influenced coastal environments: respective impact of late Holocene land use and high-frequency climate changes. *Marine Geology* 290, 51–62.
- Price, N.B., Calvert, S.E., Jones, P.G.W., 1970. Distribution of iodine and bromine in sediments of the south western Barents Sea. *Journal of Marine Research* 28, 22–34.
- Rhew, R.C., Miller, B.R., Bill, M., Goldstein, A.H., Weiss, R.F., 2002. Environmental and biological controls on methyl halide emissions from southern California coastal salt marshes. *Biogeochemistry* 60, 141–161.
- Riera, S., Wansard, G., Juliá, R., 2004. 2000-year environmental history of a karstic lake in the Mediterranean Pre-Pyrenees: the Estanya lakes (Spain). *Catena* 55, 293–324.
- Rodrigues, R., Brandão, C., Costa, J., 2003. As cheias no Douro, ontem, hoje e amanhã. In: *Ministério das Cidades* (Ed.), *Ordenamento do território e Ambiente*. Instituto da Água, Lisboa (29 pp.).
- Rodrigues, T., Grimalt, J.O., Abrantes, F.G., Flores, J.A., Lebreiro, S.M., 2009. Holocene interdependencies of changes in sea surface temperature, productivity, and fluvial inputs in the Iberian continental shelf (Tagus mud patch). *Geochemistry, Geophysics, Geosystems* 10, 1–17.
- Saunders, J.B., 1957. Trochamminidae and certain Lituolidae (Foraminifera) from the recent brackish-water sediments of Trinidad, British West Indies. *Smithsonian Miscellaneous Collection* 134 (5), 1–23.
- Scaffeta, N., 2012. Multi-scale harmonic model for solar and climate cyclical variation throughout the Holocene based on Jupiter–Saturn tidal frequencies plus the 11-year solar dynamo cycle. *Journal of Atmospheric and Solar – Terrestrial Physics* 80, 296–311.
- Schellekens, J., Buurman, P., Fraga, I., Martínez-Cortizas, A., 2011. Holocene vegetation and hydrologic changes inferred from molecular vegetation markers in peat, Penido Vello (Galicia, Spain). *Palaeogeography, Palaeoclimatology, Palaeoecology* 299, 56–69.
- Scott, D.B., 1976. Brackish-water foraminifera from Southern California and description of *Polysaccammina ipohalina* n. Gen., n. sp. *Journal of Foraminiferal Research* 6 (4), 312–321.
- Scott, D.B., Medioli, F.S., 1978. Vertical zonations of marsh foraminifera as accurate indicators of former sea-levels. *Nature* 272, 528–531.
- Scott, D.B., Medioli, F.S., 1980. Quantitative studies of marsh foraminiferal distributions in Nova Scotia: implications for sea level studies. *Special Publication – Cushman Foundation for Foraminiferal Research* 17, 58.
- Scott, D.B., Medioli, F.S., Schafer, C.T., 2001. *Monitoring in Coastal Environments Using Foraminifera and Thecamoebian Indicators*. Cambridge University Press, USA (177 pp.).
- Shindell, D.T., Schmidt, G.A., Mann, M.E., Rind, D., Waple, A., 2001. Solar forcing of regional climate change during the Maunder Minimum. *Science* 294, 2149–2152.
- Smith, J.N., 2001. Why should we believe 210Pb sediment geochronologies? *Journal of Environmental Radioactivity* 55, 121–123.
- Steinhilber, F., Abreu, J.A., Beer, J., Brunner, I., Christl, M., Fischer, H., Heikkilä, U., Kubik, P. W., Mann, M., McCracken, K.G., Miller, H., Miyahara, H., Oerter, H., Wilhelms, F., 2012. 9,400 years of cosmic radiation and solar activity from ice cores and tree rings. *PNAS* 109, 5967–5971.
- Stine, S., 1994. Extreme and persistent drought in California and Patagonia during Medieval Time. *Nature* 369, 546–549.
- Taborda, R., Dias, J.M.A., 1991. Análise da sobre-elevação do nível do mar de origem meteorológica durante os temporais de 1978 e 1981. *Geonovas*, SI, 1 pp. 89–97.
- Trigo, R.M., Pozo-Vázquez, D., Osborn, T.J., Castro-Díez, Y., Gámis-Fortis, S., Esteban-Parra, M.J., 2004. North Atlantic Oscillation influence on precipitation, river flow and water resources in the Iberian Peninsula. *International Journal of Climatology* 24, 925–944.
- Trouet, V., Esper, J., Graham, N.E., Baker, A., Scourse, J.D., Frank, D.C., 2009. Persistent positive North Atlantic Oscillation mode dominated the medieval climate anomaly. *Science* 324, 78–80.
- Usoskin, I.G., Solanki, S.K., Kovaltsov, G.A., 2007. Grand minima and maxima of solar activity: new observational constraints. *Astronomy & Astrophysics* 471, 301–309.
- Usoskin, I., 2013. A history of solar activity over millennia. *Living Reviews in Solar Physics* 10, 1–94 (URL accessed 25th November, 2013: <http://www.livingreviews.org/lrsp-2013-1>).
- Valente, T., Fatela, F., Moreno, J., Moreno, F., Guise, L., Patinha, C., 2009. A comparative study of the influence of geochemical parameters on the distribution of foraminiferal assemblages in two distinctive tidal marshes. *Journal of Coastal Research*, SI 56, 1439–1443.
- Versteegh, G.J.M., 2005. Solar forcing of climate. 2: evidence from the past. *Space Science Reviews* 120, 243–286.
- Vicente-Serrano, S.M., Cuadrat, J.M., 2007. North Atlantic oscillation control of droughts in north-east Spain: evaluation since 1600 A.D. *Climatic Change* 85, 357–379.
- Wanner, H., Beer, J., Bütikofer, J., Crowley, T., Cubasch, U., Flückiger, J., Goosse, H., Grosjean, M., Joos, F., Kaplan, J., Küttel, M., Müller, S., Prentice, I., Solomina, O., Stocker, T., Tarasov, P., Wagner, M., Widmann, M., 2008. Mid- to Late Holocene climate change: an overview. *Quaternary Science Reviews* 27, 1791–1828.
- Yamada, Y., 1968. Occurrence of bromine in plants and soil. *Talanta* 15, 1135–1141. <http://snirh.pt> (18th June 2012).
- <http://drought.unl.edu> (22th May 2013).
- IPMA, 2013. http://www.ipma.pt/pt/oclima/observatorio.secas/spi/apresentacao/evolu_historica/ (5th June 2013).
- WDC and NOAA, 2013. ftp://ftp.ncdc.noaa.gov/pub/data/paleo/climate_forcing/solar_variability/steinhilber2009tsi.txt (25th November 2013).